Glycobiology vol. 23 no. 2 pp. 259–272, 2013
doi:10.1093/glycob/cws146
Advance Access publication on October 22, 2012

Xanthan chain length is modulated by increasing the availability of the polysaccharide copolymerase protein GumC and the outer membrane polysaccharide export protein GumB

Estela M Galván[2,†], María V Ielmini[2,5†], Yamini N Patel[3], María I Bianco[2], Esteban A Franceschini[4], Jane C Schneider[3,6], and Luis Ielpi[1,2]

[2]Laboratory of Bacterial Genetics, Fundación Instituto Leloir, IIBBA-CONICET, C1405BWE Buenos Aires, Argentina; [3]Fermentation Sciences, CP Kelco, 8225 Aero Drive, San Diego, CA 92123, USA; and [4]Grupo de Celdas de Combustible, Departamento de Física de la Materia Condensada, Centro Atómico Constituyentes, CNEA, 1650 Buenos Aires, Argentina

Received on March 2, 2012; revised on October 11, 2012; accepted on October 11, 2012

Xanthan is a polysaccharide secreted by *Xanthomonas campestris* that contains pentameric repeat units. The biosynthesis of xanthan involves an operon composed of 12 genes (*gumB* to *gumM*). In this study, we analyzed the proteins encoded by *gumB* and *gumC*. Membrane fractionation showed that GumB was mainly associated with the outer membrane, whereas GumC was an inner membrane protein. By in silico analysis and specific globomycin inhibition, GumB was characterized as a lipoprotein. By reporter enzyme assays, GumC was shown to contain two transmembrane segments flanking a large periplasmic domain. We confirmed that *gumB* and *gumC* mutant strains uncoupled the synthesis of the lipid-linked repeat unit from the polymerization process. We studied the effects of *gumB* and *gumC* gene amplification on the production, composition and viscosity of xanthan. Overexpression of GumB, GumC or GumB and GumC simultaneously did not affect the total amount or the chemical composition of the polymer. GumB overexpression did not affect xanthan viscosity; however, a moderate increase in xanthan viscosity was achieved when GumC protein levels were increased 5-fold. Partial degradation of GumC was observed when only that protein was overexpressed; but co-expression of GumB and GumC diminished GumC degradation and resulted in higher xanthan viscosity than individual GumB or GumC overexpression. Compared with xanthan from the wild-type strain, longer polymer chains from the strain that simultaneously overexpressed GumB and GumC were observed by atomic force microscopy. Our results suggest that GumB–GumC protein levels modulate xanthan chain length, which results in altered polymer viscosity.

Keywords: membrane protein / polysaccharide chain length / xanthan / *Xanthomonas campestris*

Introduction

The Gram-negative bacterium *Xanthomonas campestris*, a pathogen of cruciferous plants, produces an exopolysaccharide (EPS) called xanthan. Xanthan is a polymer of repeating pentasaccharide units with a cellulose backbone and a trisaccharide side chain of two mannoses and one glucuronate residue (Jansson et al. 1975). The mannose residues are acetylated and pyruvylated to varying degrees at specific sites (Cadmus et al. 1976; Stankowski et al. 1993). Because of its ability to form viscous solutions, xanthan is used commercially as a thickening agent in the nutritional and pharmaceutical industries (Becker and Vorholter 2009). The highly hydrated and anionic consistency of xanthan protects the bacteria from environmental stresses. Moreover, xanthan contributes to bacteria *in planta* growth (Yun et al. 2006) and has a role in biofilm formation (Dow et al. 2003). The production of xanthan is directed by several genetic loci including the *gum* gene cluster, which consists of 12 genes (*gumB* to *gumM*) (Capage et al. 1987; Katzen et al. 1996).

Like most bacterial surface heteropolysaccharides, xanthan is synthesized through a Wzy-dependent pathway, which is also used for the biosynthesis of several EPS (e.g. *Acinetobacter lwoffii* emulsan, *Sinorhizobium meliloti* succinoglycan), *Escherichia coli* type 1 and 4 capsular polysaccharides (CPS) and lipopolysaccharide O-antigen (LPS O-Ag) in many species (e.g. *E. coli*, *Salmonella enterica* and *Pseudomonas aeruginosa*) (Guo et al. 2008). In this pathway, lipid-linked

[1]To whom correspondence should be addressed: Fundación Instituto Leloir. Av. Patricias Argentinas 435, C1405BWE Buenos Aires, Argentina. Tel: +54-5238-7500; Fax: +54-5238-7501; e-mail: lielpi@leloir.org.ar
[†]Both authors contributed equally to this work.
[5]Present address: M.V. Ielmini, Alberta Ingenuity Centre for Carbohydrate Sciences, Department of Biological Sciences, University of Alberta, Edmonton, AB, T6G 2E9, Canada.
[6]Present address: J.C. Schneider, Synthetic Genomics, 11149 N. Torrey Pines Rd, La Jolla, CA 92037, USA.

repeat units are built up on polyisoprenol phosphate at the cytoplasmic face of the inner membrane (IM) by the sequential activity of glycosyltransferases. The lipid-linked repeat units are then flipped to the periplasmic face of the IM by a flippase, and polymerization of the units occurs by a block-transfer mechanism that minimally involves the polymerase Wzy (Kanegasaki and Wright 1970; Woodward et al. 2010). The polysaccharide chain grows at the reducing end and, once this process is complete, it can be attached to an anchor (e.g. a lipid A-core for LPS O-Ag biosynthesis) or exported to the extracellular environment, where it can be attached to the bacterial surface as CPS or released as EPS. In Gram-negative bacteria, the Wzy-dependent polymerization and export of CPS and EPS are indistinguishable (Cuthbertson et al. 2009). These processes have been better studied for *E. coli* type 1 CPS and the EPS colanic acid. In these cases, along with the Wzy polymerase, the expression of three conserved proteins, Wza, Wzb and Wzc, is required (Stevenson et al. 1996; Wugeditsch et al. 2001). Wza is an outer membrane polysaccharide export (OPX) lipoprotein that contains the characteristic polysaccharide export sequence (PES) motif (Pfam 02563) (Drummelsmith and Whitfield 2000; Cuthbertson et al. 2009). This protein has been reported to form a homo-octameric helical barrel with a central cavity that allows the export of K30 CPS across the OM (Dong et al. 2006). Wzc is an IM polysaccharide co-polymerase (PCP) protein with a large periplasmic loop flanked by two transmembrane regions, a proline- and glycine-rich domain overlapping the second transmembrane region, and a C-terminal cytoplasmic domain that possesses an adenosine 5′-triphosphate binding site and tyrosine autokinase activity (Wugeditsch et al. 2001). Wzb is the cognate phosphatase that dephosphorylates Wzc. The interaction between a Wza octamer and a Wzc tetramer would create a molecular machine that is utilized in the export of CPS from the periplasm to the cell surface (Collins et al. 2007).

Proteins involved in xanthan repeat unit synthesis (GumDFGHIKLM) have been established on the basis of experimental data (Ielpi et al. 1993; Katzen et al. 1998; Barreras et al. 2004, 2008; Salinas et al. 2011); however, polymerization and export of xanthan is not yet well understood. It was shown that the inactivation of *gumB*, *gumC*, or *gumE* in *X. campestris* impaired xanthan production, but those mutations did not affect lipid-linked repeat unit synthesis (Katzen et al. 1998; Vojnov et al. 1998). Additionally, our preliminary studies suggested that an increase of *gumB* and *gumC* gene products relative to other genes in their operon, yields xanthan molecules of higher molecular length than when xanthan is made by wild-type cells (Patel et al. 2008). On the basis of in silico analysis, GumE, GumC and GumB have been proposed as the polymerase, the PCP protein and the OPX protein, respectively (Vorholter et al. 2008; Cuthbertson et al. 2009). Like Wza, GumB contains the PES motif characteristic of OPX proteins, but the overall primary sequence similarity between GumB and Wza is not significant. GumC has a predicted membrane topology similar to that of Wzc, except that GumC does not have a C-terminal cytoplasmic region with tyrosine autokinase activity, and no kinase polypeptide partner could be identified on the *Xanthomonas* chromosome (Cuthbertson et al. 2009). In this report, we characterize the GumB and GumC proteins and uncover the role that these proteins play in the polymerization and secretion processes of xanthan. Furthermore, gene dosage experiments have brought insights into polysaccharide length control.

Results

Characterization of the GumB and GumC proteins

Wild-type *X. campestris* FC2 (XcFC2) cells were analyzed for the expression of GumB and GumC proteins during cell growth by western blotting. Proteins of 23 and 53 kDa size were specifically detected with anti-GumB and anti-GumC antibodies, respectively, at all analyzed times (2–31 h of culture) (Figure 1A). The expression levels of both GumB and GumC did not appreciably change over time. Next, we determined the subcellular localization of GumB and GumC in the bacterium. Upon cell fractionation, GumB and GumC were exclusively detected in the membrane fraction of XcFC2 cells by western blotting (Figure 1B). Coomassie blue staining of total membranes separated by sodium dodecyl sulfate–polyacrylamide gel electrophoresis (SDS–PAGE) detected neither GumB nor GumC, indicating low expression levels of both proteins (not shown). To test whether GumB and GumC associated with the IM or the OM, we performed a sucrose sedimentation gradient of the membrane fraction. The determination of NADH oxidase activity and 2-keto 3-deoxyoctanoic acid as markers of IM and OM, respectively, demonstrated that a successful separation of both membranes was achieved (Figure 1C). By western blotting, GumC was found in the IM fraction, whereas GumB was distributed along the gradient and was particularly enriched in the OM fraction.

The *gumB* sequence originally reported (GenBank U22511) encoded a 213 amino acid protein. This protein possesses the PES motif characteristic of OPX proteins but did not present a signal sequence for targeting to the membrane. As previously noted by Paulsen et al. (1997), this GumB may be N-terminally truncated because of a sequencing error. We sequenced the *gumB* gene and its upstream region in XcFC2 and found one base deletion and one base inversion (for details, see the Materials and methods section). Searching for open reading frames in this new sequence with the Clone Manager 7, v.7.11 software (Scientific & Educational Software, NC) revealed two putative initiation codons located 55 and 232 bp upstream of the previously reported initiation codon. The ATG located 232 bp upstream was rejected because it is located in the promoter region of the *gum* operon (Katzen et al. 1996), and it codes for a 286 amino acid protein (estimated an MW of 31.3 kDa) predicted to have a cytoplasmic localization (PSORTb v3.0.2 software) (Yu et al. 2010). The initiation codon located 55 bp upstream of the previously described one codes for a GumB protein with an N-terminal extension of 19 amino acids (Figure 1D). LipoP 1.0 software (Juncker et al. 2003) predicted a consensus signal peptidase II cleavage site following a putative signal sequence in the first 24 amino acids of the N-terminus (Figure 1D), a feature characteristic of bacterial lipoproteins (Tokuda 2009). Moreover, the presence of a serine at position +2 following the acylated cysteine residue indicates OM

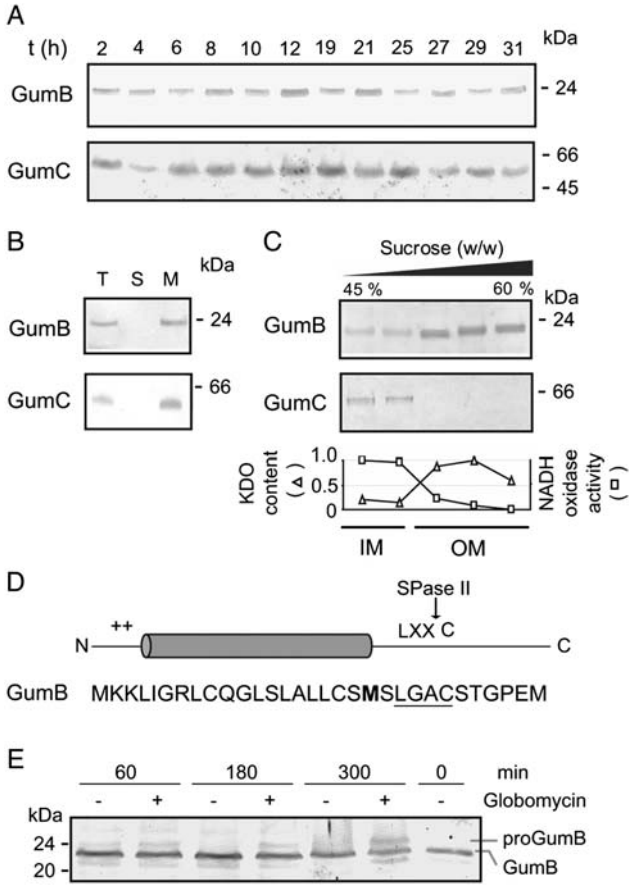

Fig. 1. Characterization of the GumB and GumC proteins. (**A**) Protein expression. XcFC2 cells were grown in XOL-SSF media at 28°C. Samples were taken at the indicated time points and subjected to western blotting using anti-GumB and anti-GumC antibodies. (**B**) Subcellular localization. Total XcFC2 cells (T) were broken by a French press; soluble (S) and membrane (M) fractions obtained after centrifugation were analyzed by western blotting using anti-GumB and anti-GumC antibodies. (**C**) Total membranes were separated on a sucrose gradient, and the collected fractions were analyzed by western blotting using anti-GumB and anti-GumC antibodies. NADH oxidase activity (squares) and 2-keto 3-deoxyoctanoic acid (KDO) content (triangles) of the fractions are represented relative to fractions having the highest values (4.06 nmol min^{-1} mg $protein^{-1}$ for the enzymatic activity and 120.0 nmol mg $protein^{-1}$ for KDO). Positions of the IM- and OM-containing fractions are indicated. (**D**) Presence of a lipoprotein signal peptide on the N-terminal sequence of GumB (AAL28080). The positively charged N-terminal region (+), the central hydrophobic domain (grey cylinder), the consensus sequence (underlined) and the site of cleavage (vertical arrow) for signal peptidase II (SPase II) processing are indicated. The initial methionine (M) of the previously reported GumB sequence is shown in bold. (**E**) GumB is a lipoprotein. Samples of XcFC2 cells treated (+) or not treated (−) with globomycin were subjected to western blotting using anti-GumB antibody. The unprocessed form of GumB is indicated as proGumB. Related molecular weight markers are indicated.

targeting. This result is in agreement with the observed GumB localization. To obtain experimental evidence for the actual translational start of *gumB*, both the original and 53 bp extended open reading frames were introduced *in trans* into the *gumB* mutant strain Xc3192B. Xanthan biosynthesis would be indicative of the restoration of GumB activity. As

Table I. Synthesis of lipid-linked pentasaccharide and polysaccharide in *gumB* and *gumC* mutant strains

Strain	In vitro[a] (pmol [^{14}C]GlcA mg^{-1})		In vivo[b,c] (g 100 mL^{-1})
	Lipid-bound pentasaccharide	Polymer	Polymer
Xc3192	69.8 ± 4.6	68.7 ± 10.9	1.09 ± 0.12
Xc3192B	66.5 ± 2.1	2.9 ± 0.1	<0.01
Xc3192B/pBBad-B	n.d.	n.d.	1.06 ± 0.06
Xc3192B/pBBR-promB	n.d.	n.d.	1.13 ± 0.15
Xc3192B/pBBR-promB$_{22511}$	n.d.	n.d.	<0.01
Xc3192C	60.7 ± 5.5	1.8 ± 0.3	<0.01
Xc3192C/pBBad-C	n.d.	n.d.	1.05 ± 0.07
Xc3192E	68.1 ± 4.3	1.6 ± 0.2	<0.01
Xc3192E/pBBad-E	n.d.	n.d.	1.12 ± 0.09

Each value corresponds to the mean ± SD of three independent experiments.
[a]In vitro incorporation of [^{14}C]GlcA.
[b]Polymer obtained from the culture media after 4 days growth.
[c]For in vivo determinations, strains were also complemented with pJC440 to restore sugar nucleotide synthesis.
n.d.: not determined.

explained below, inactivation of the *gumB* gene was achieved in a strain that is also deficient in uridine diphosphate (UDP)-glucose pyrophosphorylase activity (Xc3192), and consequently, the in vivo experiments of xanthan production required the introduction of pJC440 to restore UDP-Glc synthesis (Harding et al. 1993). Table I shows that plasmids carrying the extended *gumB* gene (pBBR-promB or pBBad-B) but not the plasmid carrying the previously reported sequence (pBBR-promB$_{22511}$) were able to restore xanthan production in Xc3192B.

To experimentally determine whether GumB is a lipoprotein, we evaluated the effect of globomycin, a specific signal peptidase II inhibitor (Inukai et al. 1978). We added globomycin to growing XcFC2 cells and detected GumB by western blotting. Only the mature form of the GumB protein (MW ~23 kDa) was observed in the absence of globomycin; however, after incubation of bacterial cells with globomycin, a higher molecular weight band (MW ~25 KDa) was observed (Figure 1E). Increasing amounts of the higher molecular weight band were obtained when the globomycin treatment was extended over time. Its localization to the OM, the presence of a lipoprotein signal sequence, and the accumulation of the precursor in the presence of globomycin suggest that GumB is an OM lipoprotein.

The original reported *gumC* gene sequence ((Capage et al. 1987), GenBank U22511) codes for a 449 amino acid protein. GumC from *Xylella fastidiosa* 9a5c (GenBank AAF85168) and several related proteins have ~20 extra amino acids at the N-terminus. We decided to sequence the *gumC* gene including the intergenic region between *gumB* and *gumC* from XcFC2 cells (see Materials and methods). We found a difference in one base, generating a shift in the open reading frame upstream of the previously described ATG. The GumC predicted protein sequence (AAL28079) has 23 extra amino acids at the N-terminus, resulting in a total length of 472 amino acids and estimated an MW of 53 kDa. We investigated which form of

GumC is expressed in *X. campestris* by western blotting with an anti-GumC antibody. Xc1231, a mutant strain lacking the whole *gum* operon, was transformed with pBBR-promC (which expresses a 472 amino acid-long protein) or pBBR-promC$_{22511}$ (which expresses a 449 amino acid-long protein). Xc1231/pBBR-promC showed a band that comigrated with the one detected in XcFC2 (Supplementary data, Figure S1A). On the contrary, a faster migrating protein was detected in Xc1231/pBBR-promC$_{22511}$. This result indicates that the extended form of GumC is the relevant one in *X. campestris*. A complete restoration of xanthan production to wild-type levels was observed in vivo for Xc3192C cells that were complemented with pBBad-C (which expresses the extended GumC protein) and pJC440 when the bacteria were grown in media containing 0.01% arabinose (Table I).

Proteins belonging to the PCP family share a conserved membrane topology consisting of two transmembrane segments flanking a large hydrophilic periplasmic domain (Morona et al. 2000). Based on analysis using the TMHMM v.2.0 software (Sonnhammer et al. 1998; Krogh et al. 2001), GumC has two transmembrane segments localized between amino acids L34-P56 and N440-L462 and a large hydrophilic domain of 384 amino acids. To test this prediction, we constructed targeted fusions of *gumC* to either the gene encoding the *E. coli* alkaline phosphatase (*phoA*) or β-galactosidase (*lacZ*). Reporter enzyme assays showed a 10-fold greater alkaline phosphatase activity for the *phoA* fusions located between the two predicted transmembrane regions (N135 and V343) than for the *phoA* fusion located near the C-terminus (R463) (Supplementary data, Figure S1B). The opposite result was found for the identical sites that were fused to *lacZ*. These results support the predicted topology of GumC that is in agreement with the conserved membrane topology shared by PCPs (Morona et al. 2000).

Basic Local Alignment Search Tool (BLAST) searches identified a number of homologs to GumB and GumC belonging to different Gram-negative bacteria (Supplementary data, Table SI). As expected, the top hits were from *Xanthomonas* species, with amino acid identities of 88–93% for both GumB and GumC. Proteins from *Xyllela* species are 61–66% identical to GumB and GumC, while sequences from *Mesorhizobium*, *Agrobacterium*, *Sphingomonas* and *Rhizobium* have an identity of ~33–43%.

Inactivation of gumB *or* gumC *drastically reduced xanthan production*

It was previously observed that the inactivation of *gumB*, *gumC* and *gumE* in the wild-type XcFC2 strain was followed by further chromosomal rearrangements; however, all of these genes could be mutated in the UDP-glucose deficient strain Xc3192 (Katzen et al. 1998). Xanthan synthesis was studied in vitro by incubating Ethylenediaminetetraacetic acid (EDTA)-treated *X. campestris* cells with UDP-glucose, guanine diphosphate (GDP)-mannose and UDP-[^{14}C]glucuronic acid. The incorporation of radioactivity into the polymer (i.e. the aqueous incubation supernatants) and the lipid-linked pentasaccharide fractions (i.e. the organic solvent extracts) were analyzed by gel filtration and thin layer chromatography, respectively. As expected, substantial amounts of xanthan polymer and lipid-linked pentasaccharide intermediates were obtained in vitro from permeabilized Xc3192 cells (Table I). Although *gumB* and *gumC* mutant cells synthesized lipid-linked repeat units, they only produced 2–3% of the xanthan polymer made by the parental strain. The amounts of lipid-linked pentasaccharides synthesized by the *gumB* and *gumC* mutant cells were similar to those obtained in the parental strain, suggesting that the pool of lipid intermediates is at its maximum even under conditions of active xanthan synthesis. These results suggest that biosynthesis of the pentasaccharide repeat unit could be uncoupled from the polymerization and export processes.

In vivo complementation assays confirmed that the phenotype observed in each mutant was caused by inactivation of the targeted gene and not by a downstream effect. As shown in Table I, a complete restoration of xanthan production to parental levels was observed for Xc3192B cells that were complemented with both pBBad-B and pJC440. Similarly, Xc3192C complemented with both pBBad-C and pJC440 produced the same amount of xanthan as Xc3192/pJC440. The amount of xanthan produced in vivo by Xc3192/pJC440 was lower than that produced by the XcFC2 (1.09 ± 0.12 and 2.07 ± 0.15 g per 100 mL culture, respectively). These experimental results confirmed earlier predictions on the basis of in silico analysis suggesting that the GumB and GumC functions are most likely related to processes involved in xanthan polymerization and/or secretion.

Effect of GumC overexpression on the rheological properties of xanthan

PCP proteins that participate in the biosynthesis of LPS O-Ag have been shown to regulate polymer chain length (Morona et al. 1995). To obtain insights into the putative role of GumC as a modulator of xanthan chain length, we overexpressed this protein in a wild-type background and analyzed the polymer that was produced. For this purpose, the arabinose-inducible plasmid pBBad-C was introduced into XcFC2 cells, and the cells were grown in media containing variable amounts of arabinose. Because GumC is a membrane protein, we first established the maximal amounts of this protein that a cell can tolerate without causing detrimental growth effects. Alterations of the XcFC2/pBBad-C growth curve were observed for arabinose concentrations that were equal to or higher than 0.3% (w/v) (Supplementary data, Figure S2B). Consequently, the highest inductor concentration used was 0.1% arabinose. The growth of XcFC2 cells carrying the empty vector pBBad22K (see Table II) was not affected by the arabinose added to the culture media (Supplementary data, Figure S2A). The expression levels of GumC were assessed by western blotting analysis of the total membranes isolated from XcFC2 cells carrying the pBBad-C plasmid or the empty vector, as a control. A 2-fold GumC overexpression was observed in XcFC2/pBBad-C cells not induced with arabinose, compared with wild-type cells (Figure 2A, Supplementary data, Table SII). This result is in agreement with the observed basal expression of genes cloned into pBBad plasmid derivatives when these plasmids are introduced in *X. campestris* (Sukchawalit et al. 1999). A gradual increase in GumC was obtained by growing XcFC2/pBBad-C cells in the presence of increasing concentrations of arabinose. In the presence of 0.1% arabinose, the

Table II. Bacterial strains and plasmids used in this work

Plasmid or strain	Relevant genotype and characteristics	Source of reference
X. campestris strains		
XcFC2	Rif^r derivative from wild-type NRRL B-1459	(Katzen et al. 1998)
Xc1231	NRRL B-1459 Tc::Tn10 Δ*gum*	(Capage et al. 1987)
Xc3192	NRRL B-1459 derivative *ugp* Rif^r	(Harding et al. 1993)
Xc3192B	Xc3192 carrying the plasmid pGum57-18S integrated into the genome disrupting *gumB*	This work
Xc3192C	Xc3192 Φ(*gumC-lacZ-aacC1*) insertion site: *Xmn*I (nucleotide 2556)[a] disrupting *gumC*	This work
Xc3192BC	Xc3192 Δ*gumB* Δ*gumC* (nucleotides 1276–3397[a])	This work
Xc3192E	Xc3192 Δ*gumE* (nucleotides 5629–6138[a])	This work
Plasmids		
pJC440	Plasmid based on pRK293 carrying *xpsIV* region of *X. campestris*	(Harding et al. 1993)
pGum57-18S	pK18mob containing 437-bp fragment of *gumB* (nucleotides 1372–1809)[a] Km^r	(Katzen et al. 1998)
pBBad22K	Overexpression broad-host range vector containing BAD promoter, pBBR1MCS-4 replicon, Km^r	(Sukchawalit et al. 1999)
pBBad22T	Overexpression broad-host range vector containing BAD promoter, pBBR1MCS-4 replicon, Tc^r	(Sukchawalit et al. 1999)
pBBR1-MCS-5	pBBR1-MCS derivative, mob-site, LacZα$^+$, Gm^r	(Kovach et al. 1995)
pBBR-prom	pBBR1-MCS-5 carrying *gum* promoter (1000–1276)[a]	This work
pBBad-B	pBBad22T carrying *gumB* gene (1276–1975)[a]	This work
pBBR-promB	pBBR1-MCS-5 carrying *gum* promoter and *gumB* gene (770–1979)[a]	This work
pBBR-promB$_{22511}$	pBBR-prom carrying *gumB* gene fragment (1333–1975)[a]	This work
pBBR-promC	pBBR-prom carrying *gumC* gene (1978–3397)[a]	This work
pBBR-promC$_{22511}$	pBBR-prom carrying *gumC* gene fragment (2048–3397)[a]	This work
pBBad-C	pBBad22K carrying *gumC* gene (1978–3397)[a]	This work
pBBad-BC	pBBad22K carrying *gumB* and *gumC* genes (1276–3397)[a]	This work
pBBad-E	pBBad22K carrying *gumE* gene (5175–6474)[a] followed by a C-terminal His6 tag	This work

[a]Fragment of the *gum* region. Numbers correspond to the position in the nucleotide sequence of GenBank, accession number U22511.

GumC membrane level in XcFC2/pBBad-C cells was 6-fold higher than that of XcFC2/pBBad22K cells. For all of the overexpression conditions, two additional faster migrating bands, which could correspond to degradation products of GumC, were detected with an anti-GumC antibody. It was also evident that overexpressing GumC did not have any effect on the levels of GumB expression.

Next, xanthan production and viscosity were determined. XcFC2/pBBad-C cells grown in the presence of increasing concentrations of inducer (i.e. 0–0.1% arabinose) produced similar amounts of xanthan compared with XcFC2 cells that carried the empty vector (~2.00 g per 100 mL culture media). The sugar compositions of the polymers were analyzed by ^{1}H-nuclear magnetic resonance (NMR) spectroscopy after acid hydrolysis of the samples. We found that the ratios of glucose, mannose, glucuronic acid and pyruvate remained similar to the control xanthan in all cases (Supplementary data, Figure S3). Determinations of the low shear rate viscosities of xanthan samples indicated that most of the GumC overexpression conditions assayed did not significantly affect the polymer viscosity (Figure 2B). Only xanthan isolated from XcFC2/pBBad-C cells cultured in the presence of 0.03% arabinose showed a 2-fold increase in low shear rate viscosity. Furthermore, the intrinsic viscosity was higher for this xanthan sample than for the wild-type XcFC2 sample (increase of 22%) (Table III). The intrinsic viscosity is directly proportional to the molecular weight of the polymer as long as it is measured under identical solvent and temperature conditions ($[\eta] = K \times M_r^a$, Mark–Houwink–Sakurada equation) (Hiemenz and Lodge 2007). This result suggests that a higher molecular weight xanthan (i.e. longer chains) is produced by XcFC2 cells where GumC is overexpressed.

Co-overexpression of GumB and GumC modulate xanthan chain length

In *E. coli*, both the PCP and OPX proteins play a role in the polymerization and export of type 1 and type 4 CPS (Cuthbertson et al. 2009). We explored the effects of GumB and GumC expression levels on the chain length of xanthan produced by wild-type *X. campestris*. First, we introduced the arabinose-inducible plasmid pBBad-BC, which carried the *gumB* and *gumC* genes *in tandem*, into XcFC2 cells. Similarly to XcFC2/pBBad-C cells, 0.1% arabinose was the highest amount of inducer that did not dramatically affect the growth of XcFC2/pBBad-BC cells (Supplementary data, Figure S2C). Bacterial membranes analyzed by western blotting showed that GumB and GumC levels increased as the inducer concentration was increased from 0 to 0.1% arabinose (Figure 3A). Bacteria grown in the presence of 0.1% arabinose produced the highest overexpression levels of GumB and GumC (5- and 7-fold, respectively) (Supplementary data, Table SII). The two smaller-sized bands, which corresponded to degraded GumC products detected in XcFC2/pBBad-C cells, were also observed in the XcFC2/pBBad-BC cells; however, the intensity of these bands was significantly lower at high inducer concentrations. This result suggests that GumB is involved in GumC stabilization.

The evaluation of xanthan production indicated that similar amounts of polymer were produced independently of the levels of GumB and GumC expression (~2.00 g per 100 mL culture media). Nevertheless, viscosity determinations indicated that the quality of these polymer samples was different. Xanthan isolated from cells overexpressing *in tandem* increasing amounts of both GumB and GumC showed a gradual increase in low shear rate viscosity (Figure 3B). The highest viscosity (i.e. a 3.5-fold increase over the control xanthan) was achieved

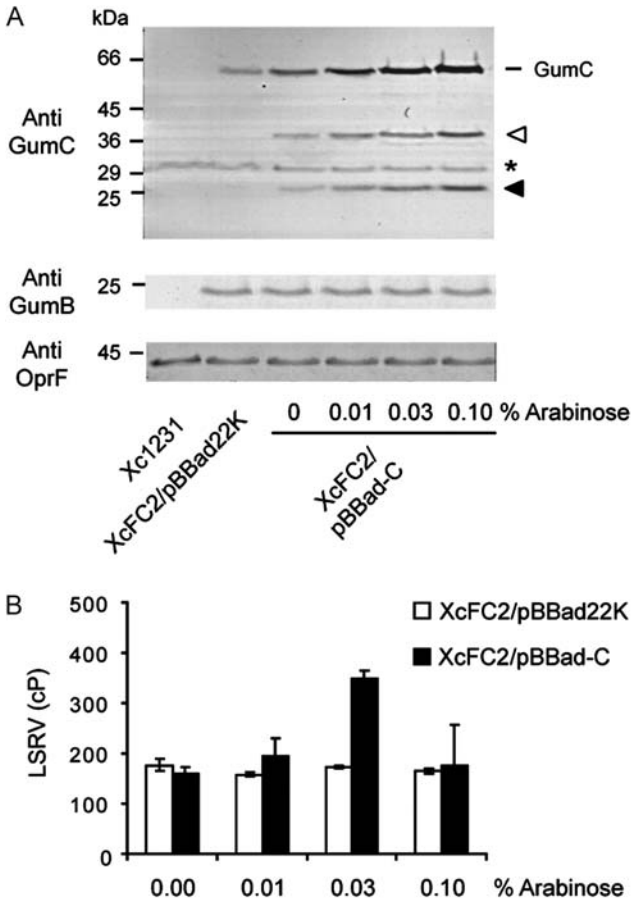

Fig. 2. GumC overexpression and its effect in xanthan viscosity. (**A**) Expression levels of GumC and GumB. Equivalent amounts of total membrane proteins isolated from XcFC2/pBBad-C or XcFC2/pBBad22K, induced or not induced with arabinose, were analyzed by western blotting with anti-GumC and anti-GumB antibodies. Anti-OprF antibody was used as an internal control to detect the amount of membrane loaded into each lane. Membranes from the Xc1231 strain (which carries a deletion of the entire *gum* operon) were used as negative control. Open and filled arrowheads indicate GumC degradation products, and the asterisk indicates a nonspecific band recognized by the anti-GumC antibody. Positions of related molecular weight markers are indicated. (**B**) Viscosity of xanthan produced by *X. campestris* overexpressing GumC. Xanthan from XcFC2/pBBad-C was isolated after the bacteria were grown in medium containing varying amounts of arabinose. Low shear rate viscosities (LSRV) of 0.45% (w/v) xanthan solutions were determined. Each bar represents the mean ± SD of three independent experiments.

Table III. Intrinsic viscosity [η] of xanthan produced by XcFC2 cells overexpressing GumC or GumB–GumC

Strain	Arabinose[a] (%)	[η]	
		(dL g^{-1})	%[b]
XcFC2/pBBad22K	0.10	14.8	100
XcFC2/pBBad-C	0.03	18.1	122
XcFC2/pBBad-BC	0.10	21.8	147

[a]Arabinose concentration added to the bacterial culture media.
[b]Percentage with respect to wild-type strain.

in under where the maximal expression of GumB and GumC occurred. Moreover, we observed a 47% increase in the intrinsic viscosity of this xanthan sample compared with the wild-

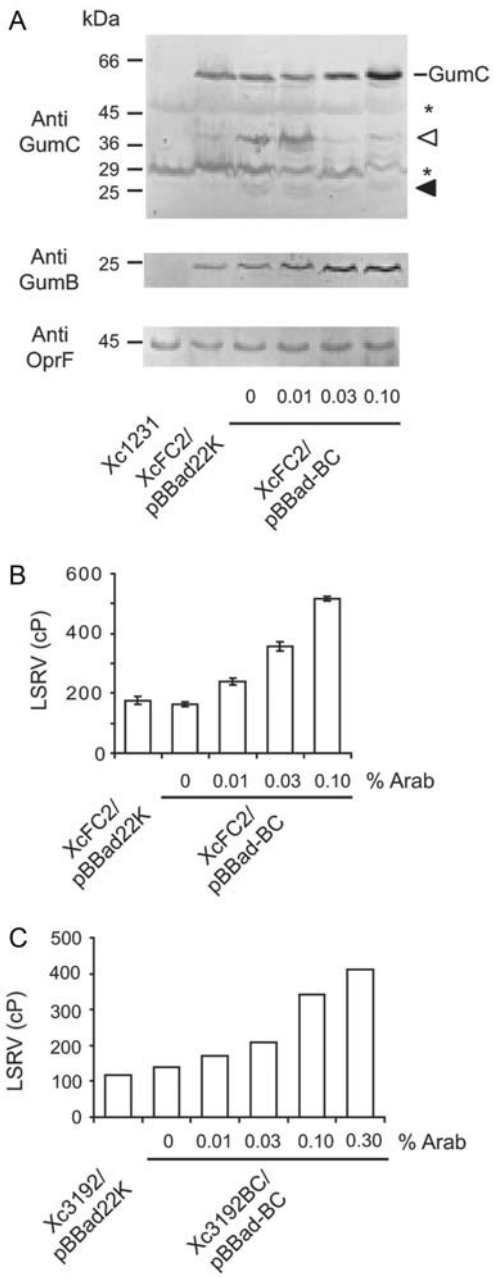

Fig. 3. Co-expression of GumB and GumC increased xanthan viscosity. (**A**) Expression levels of GumC and GumB in XcFC2 cells carrying pBBad-BC and grown in the presence of increasing arabinose concentrations. Bacterial membranes were analyzed by western blotting, as indicated in the legend of Figure 2. Arrowheads indicate GumC degradation products and asterisks indicate nonspecific bands. (**B**) LSRV of xanthan samples obtained from XcFC2/pBBad-BC cells. Determinations were performed as indicated in the legend of Figure 2. Each bar represents the mean ± SD of three independent experiments. (**C**) LSRV of xanthan samples obtained from Xc3192BC transformed with pBBad-BC and pJC440 and grown with increasing arabinose concentrations. Each bar represents the mean of two independent experiments, with less than a 10% difference between each determination.

type sample (Table III). The sugar composition of the polymers obtained from cells overexpressing GumB and GumC, as analyzed by ^{1}H NMR spectroscopy, indicated no differences between them (Supplementary data, Figure S3).

Next, we studied whether the co-expression of GumB and GumC through individual plasmids would also affect xanthan low shear rate viscosity. Xanthan from XcFC2 carrying both pBBad-B and pBBad-C grown in the presence of 0.1% arabinose showed a 2.9-fold higher viscosity than xanthan from XcFC2 cells carrying the empty vectors (440 vs. 152 cP, respectively), revealing a similar effect of GumB and GumC co-expression and *in tandem* expression.

Finally, to examine the effect of GumB and GumC expression on xanthan chain length from a null baseline, we constructed a double *gumB gumC* mutant strain. As occurred for the single mutants, this double mutation was obtained in the UDP-Glc-deficient strain Xc3192 (generating Xc3192BC); inactivation of both *gumB* and *gumC* genes in the wild-type strain XcFC2 was unsuccessful. Xc3192BC was not able to produce xanthan in vivo when UDP-Glc synthesis was restored by introduction of pJC440. Plasmid pBBad-BC along with pJC440 fully complemented Xc3192BC, as evidenced by in vivo xanthan production (1.2 ± 0.1 vs. 1.1 ± 0.1 g xanthan in 100 mL culture of Xc3192BC/pJC440/pBBad-BC and Xc3192/pJC440, respectively). In the absence of arabinose, Xc3192BC/pJC440/pBBad-BC expressed similar levels of GumB and GumC similar to those by the control strain Xc3192/pJC440 (Supplementary data, Table SII). Moreover, the amount of polymer produced (1.2 ± 0.1 g/ 100 mL) and its viscosity (Figure 3C) were comparable with the control strain. Figure 3C also showed that increasing arabinose concentrations in the cell culture caused a gradual increase in xanthan low shear rate viscosity. This effect correlated with the increasing amounts of GumB and GumC detected in the bacterial membranes (Supplementary data, Table SII). The highest viscosity (i.e. a 3.2-fold increase over the control xanthan) was achieved for xanthan produced under conditions of maximal induction (0.3% arabinose in the culture). In this condition, no GumC degradation was noticeable (not shown), and the levels of GumB and GumC overexpression, determined after western blotting analysis, were 4.8- and 6.2-fold, respectively (Supplementary data, Table SII).

We confirmed that the increase in xanthan viscosity was the presence of longer polymer molecules by direct observation of individual chains using atomic force microscopy. The average contour length (i.e. the total stretched-out length of the chain) for xanthan obtained from XcFC2/pBBad-BC cells grown in the presence of 0.1% arabinose was significantly higher than that obtained from XcFC2/pBBad22K cells (0.78 and 0.46 µm, respectively) (Figure 4). Under our experimental conditions, 61% of the xanthan chains from the XcFC2/pBBad22K cells had a size of up to 0.50 µm, while only 34% of the molecules produced by the XcFC2/pBBad-BC cells were in this range. In addition, we observed a higher proportion of molecules between 1.00 and 2.00 µm in xanthan from the strains overexpressing GumB and GumC compared with the wild-type strain (19.5 and 5.8%, respectively).

No effect on xanthan viscosity (Figure 5B) or composition (Supplementary data, Figure S3) was observed when only the overexpression of GumB was studied. However, the level of membrane-localized GumB increased up to 4.5-fold under these conditions (Figure 5A, Supplementary data, Table SII).

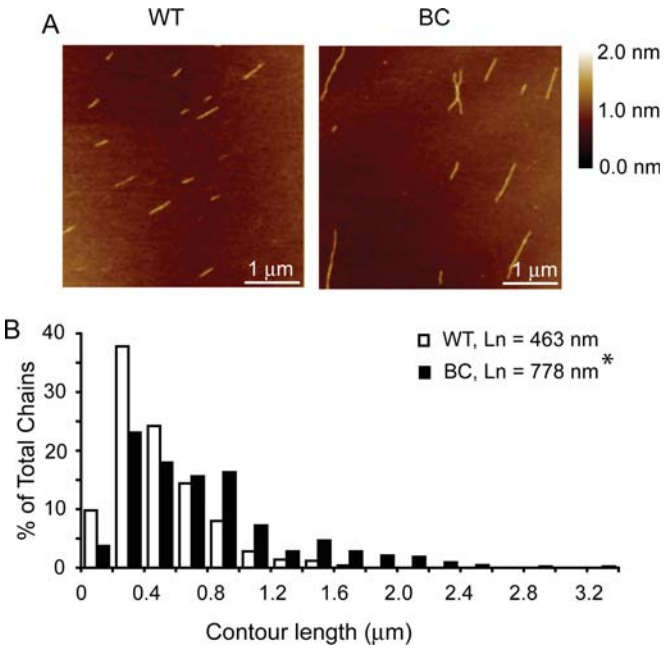

Fig. 4. Longer xanthan chains are produced by *X. campestris* cells co-overexpressing GumB and GumC. (**A**) Atomic force microscopy of xanthan molecules. Representative images of xanthan chains from XcFC2/pBBad22K (WT, left panel) and XcFC2/pBBad-BC (BC, right panel). Xanthan isolated from culture media of bacteria grown in the presence of 0.1% arabinose. (**B**) Contour length distribution of xanthan chains from wild-type XcFC2 cells carrying the empty vector (white bars) or pBBad-BC (black bars). The number average contour length (Ln) for each strain is indicated. In each case, the length of at least 450 molecules was measured. (*) Significant difference compared with the wild-type strain, Student's *t*-test $P < 0.001$.

GumE overexpression diminished xanthan viscosity

Considering that xanthan polymerization and export seem to be linked, we looked at the role of the putative polymerase GumE in xanthan biosynthesis. In silico analysis showed that *gumE* open reading frame coded for a 432 amino acid-long protein that is predicted to possess ten transmembrane regions, two major and two minor hydrophilic loops, and to be localized in the IM (Supplementary data, Figure S1C). BLAST analysis identified homologs to GumE among *Xanthomonas* and *Xyllela* species (with amino acid identities of ~88 and 62%, respectively) (Supplementary data, Table SI). Contrary to the results observed for GumB and GumC, no hits were found in other species, with the exception of *Rhizobium leguminosarum* (27% amino acid identity). As shown in Table I, in vitro experiments with permeabilized cells showed that the *gumE* mutant strain Xc3192E did not polymerize the pentasaccharide repeating units. To demonstrate that the abrogation of xanthan production in the *gumE* mutant strain was due solely to inactivation of the *gumE* gene, we complemented the phenotype by introducing a copy of the *gumE* gene *in trans*. In vivo complementation of Xc3192E with pBBad-E, together with pJC440

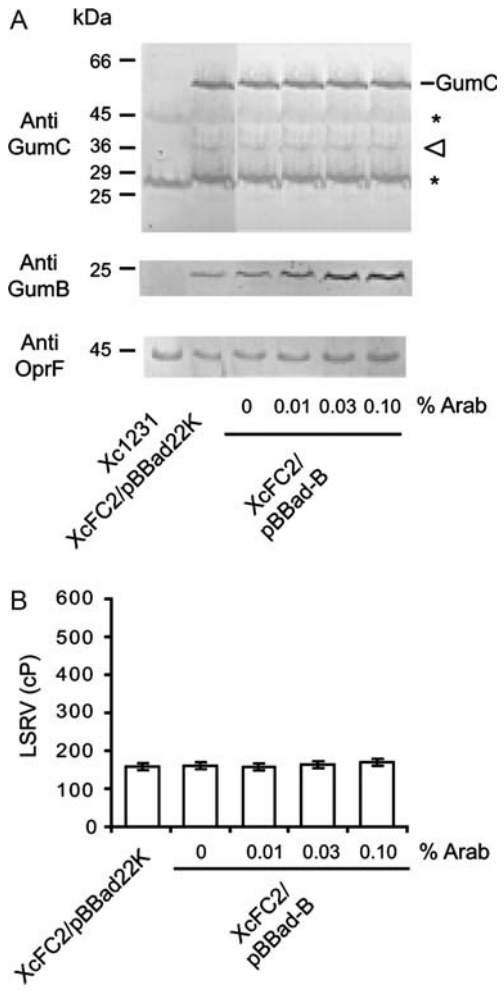

Fig. 5. GumB overexpression does not affect xanthan viscosity. (**A**) Expression levels of GumC and GumB in XcFC2 cells carrying pBBad-B after being grown in the presence of increasing arabinose concentrations. Bacterial membranes were analyzed by western blotting, as indicated in the legend of Figure 2. (**B**) LSRV of xanthan samples obtained from XcFC2/pBBad-B cells. Determinations were performed as indicated in the legend of Figure 2. Each bar represents the mean ± SD of three independent experiments.

to restore sugar nucleotide synthesis, restored xanthan production to parental levels. This occurred even without adding arabinose to induce GumE expression through pBBad-E, indicating that a basal level of GumE expression is driven by pBBad-E into *X. campestris*. We failed to detect this GumE protein, which carries a C-terminal His_6 tag, on bacterial membranes subjected to western blotting using a monoclonal anti-His antibody. Unfortunately, several attempts to overexpress enough amounts of GumE, either in *E. coli* or *X. campestris*, to generate an anti-GumE antibody were unsuccessful. In this regard, Wzy polymerases have been reported to be scarcely expressed in the bacterial membranes (Daniels et al. 1998; Carter et al. 2009). It is worth mentioning that in the case of Wzy of *E. coli* O86, a successful expression has been achieved using a chaperone coexpression system (Woodward et al. 2010).

We looked at the effect of GumE overexpression on xanthan chain length by determining xanthan viscosity. We observed that XcFC2/pBBad-E produced a polymer with 60% lower viscosity compared with XcFC2/pBBad22K (82 ± 6 vs. 184 ± 13 cp, respectively) when no arabinose was added. This polymer did not show any difference in its chemical composition compared with xanthan obtained from the wild-type strain (Supplementary data, Figure S3). No difference in GumB and GumC protein levels was observed compared with XcFC2 (Supplementary data, Table SII). This result suggests that under the conditions we used, additional copies of *gumE* reduced the length of xanthan chains. Further investigations regarding the effect of increasing *gumE* dosage on xanthan chain length would require the ability to determine the membrane levels of GumE being expressed.

Discussion

The polymerization and export of bacterial extracellular polysaccharides are poorly understood processes. In the case of xanthan biosynthesis, the GumB, GumC and GumE proteins have been proposed to be involved in these processes (Katzen et al. 1998; Vojnov et al. 1998). In silico analysis suggested that GumB is a member of the OPX family, on the basis of the presence of the characteristic PES motif (Pfam 02563) (Cuthbertson et al. 2009). The GumB protein we reported on this study has a 19 amino acid-long signal peptide typical of bacterial lipoproteins (Tokuda 2009). The membrane localization and processing by signal peptidase II experimental data support the idea that GumB is an outer membrane (OM) lipoprotein. A small amount of GumB was also detected in IM fractions. It might be possible that GumB was retained in these fractions through an interaction with GumC if a protein complex involving GumB and GumC is formed, similar to the complex observed for *E. coli* Wza and Wzc (Collins et al. 2007). Our attempt to detect GumB-acylation with [^{3}H]palmitate in *X. campestris* was unsuccessful (not shown). Additional experiments will be needed to identify the acyl chains on GumB. It was reported in *Rhizobium leguminosarum* that palmitoylation of the OPX protein PssN could not be detected in the wild-type TA1 strain but was observed in *E. coli* expressing recombinant PssN (Marczak et al. 2006). Reporter enzyme and membrane localization assays demonstrated that GumC is an IM protein with a topology consisting of two transmembrane segments flanking a large periplasmic domain. This topology is shared by all PCP proteins (Morona et al. 2000).

We confirmed that inactivation of *gumB*, *gumC* or *gumE* in *X. campestris* abolished the ability of the bacteria to produce xanthan polymer without affecting the synthesis of the lipid-linked repeat unit. These findings suggest that lipid-linked pentasaccharide synthesis can be uncoupled from the polymerization and translocation of xanthan chains (Figure 6). We observed that *gumB*, *gumC* and *gumE* mutant strains made no detectable xanthan in vivo; however, a very small amount of polymer was detected in vitro. Although this observation might be reflecting that a small level of pentasaccharide repeat unit polymerization still occurs when *gumB*, *gumC* or *gumE* are inactivated, we cannot rule out the

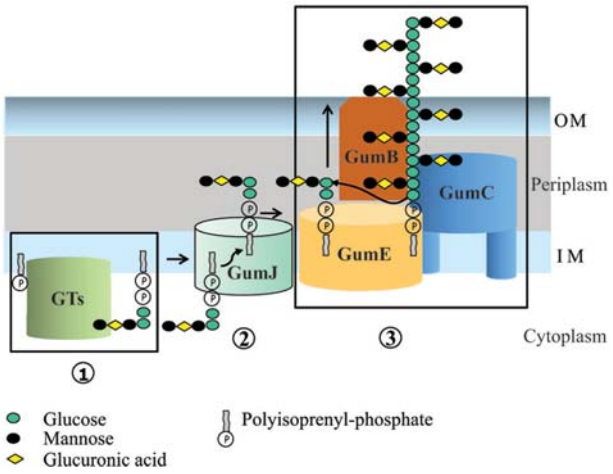

Fig. 6. Proposed pathway of xanthan biosynthesis. Step 1, glycosyltransferases synthesize the lipid-linked repeat units at the cytoplasmic face of the IM. Step 2, the lipid-linked repeat units are flipped across the IM. Step 3, the repeat units are polymerized and exported by a concerted process requiring GumE (the polymerase), GumC (the PCP) and GumB (the OPX).

possibility that some other EPS is made by these mutants. There is evidence for polysaccharides other that xanthan generated by *X. campestris* (Tao et al. 2010). We speculate that all the three GumB, GumC and GumE proteins are needed for both polysaccharide polymerization and export. Many Gram-negative bacteria that synthesize EPS/CPS via a Wzy-dependent mechanism showed the same phenotype for the null mutants of the corresponding OPX and PCP proteins: Impairment of polymer production (Reuber and Walker 1993; Huang and Schell 1995; Drummelsmith and Whitfield 2000; Mazur et al. 2002; Reid and Whitfield 2005).

PCP-1 proteins, such as Wzz, have been shown to influence the chain length of the LPS O-Ag (Morona et al. 1995; Raetz and Whitfield 2002); however, it is not clear whether PCPs are chain length regulators of EPS/CPS assembly. To investigate whether GumC modulates xanthan length, *gumC*-overexpressing strains were studied. The polymer length of xanthan from strains expressing variable amounts of GumC was first assessed by measuring the viscosity of xanthan solutions. The similar chemical composition of all of the samples obtained, particularly the ketal pyruvate content, allowed us to assume a direct relationship between viscosity and xanthan chain length. When overexpressed alone, variable levels of GumC resulted either in a moderate or in no increase in xanthan viscosity. In these experiments, partially degraded GumC was found. Considering that PCP proteins are known to oligomerize (Collins et al. 2006; Tocilj et al. 2008), we speculate that GumC degradation products present in the bacterial membrane together with the full-length protein could interfere with the formation of additional, functional GumC oligomers. In contrast, concomitant expression of GumB and GumC produced a gradual increase in xanthan viscosity that correlated with the increasing levels of both proteins. Atomic force microscopy of individual chains confirmed the presence of a significant number of longer molecules in xanthan samples from cells overexpressing GumB and GumC, compared with those from wild-type cells. A similar effect was observed for a *X. campestris* production strain, XWCM1. When this strain overexpressed GumB and GumC by introduction of pBBR5-BC (a plasmid containing the *gum* promoter that drives *in tandem* expression of *gumB* and *gumC*), a significant number of xanthan molecules with higher molecular length than those from the wild-type strain were synthesized (Patel et al. 2008).

How the concomitant overexpression of GumB and GumC leads to a shift in the size distribution of xanthan is not clearly understood. We observed that co-expression of both GumB and GumC strongly reduced GumC degradation. Because our co-expression system kept the ratio GumB: GumC similar to the ratio observed for wild-type *X. campestris*, we speculate that GumB and GumC might interact to make a protein complex that is less susceptible to the action of periplasmic proteases than the individual proteins. The formation of a protein complex between an OPX and a PCP protein has been shown in the *E. coli* K30 strain, where Wza and Wzc oligomers interact making a complex that spans the periplasm and connects the IM and the OM (Collins et al. 2007). Contrary to our observations, it has been reported that the level of expression of the PCP protein Wzz does not affect LPS O-Ag chain length (Kintz and Goldberg 2011). Several differences between Wzz and GumC suggest that their mechanism of action might be different. Phylogenetic analysis of the predicted periplasmic regions of PCP proteins involved in CPS/EPS biosynthesis classified GumC as a PCP2a-like protein, closer to PCP2a proteins (such as Wzc) than to PCP1 proteins (Wzz homologs) (Cuthbertson et al. 2009). Moreover, Wzz proteins have smaller periplasmic domains (240–280 amino acids) than PCP2a proteins (360–400 amino acids). These sizes correlate with the sizes of the polysaccharides they synthesize; while LPS O-Ag carries 10–100 oligosaccharide repeat units, CPS and EPS are large polysaccharides composed of several hundreds to several thousands oligosaccharide repeat units. In particular, GumC is predicted to have a 382 amino acid-long periplasmic domain, and xanthan chains are comprised of an average of 2000 pentasaccharide repeat units. Moreover, proteins needed for the last steps of LPS O-Ag and CPS/EPS polysaccharide biosynthesis are different. While the functions of LPS O-Ag polymerase (Wzy), co-polymerase (Wzz) and ligase (WaaL) have been well differentiated (Raetz and Whitfield 2002), polymerization and export seem to be linked in CPS/EPS biosynthesis. In the case of xanthan synthesis, these processes involve the putative polymerase GumE, the PCP GumC and the OPX GumB acting in concert. On the other hand, most PCP2 proteins have a C-terminal cytoplasmic domain with tyrosine autokinase activity, and its phosphorylation state seems to be important for PCP2 function. In this regard, a report on the biosynthesis of the EPS emulsan from *Acinetobacter lwoffii* RAG-1 proposed a model in which phosphorylation-dephosphorylation of the PCP2a protein Wzc regulates the polymerization, transport and release of emulsan, establishing the size of the released polymer (Nakar and Gutnick 2003). However, this type of regulation is not possible for GumC because it lacks the cytoplasmic C-terminal kinase domain and no kinase polypeptide partner could be identified on the *Xanthomonas* chromosome.

We speculate that the ratio between GumB, GumC and GumE modulates the polymerization reaction, determining the length of the exopolysaccharide. As discussed above, the ratio between GumB and GumC seems to be crucial to GumC stability, and an imbalance toward higher levels of GumC generated substantial GumC degradation. Concomitant overexpression of GumB and GumC in wild-type *X. campestris* cells could be interpreted as an alteration in the ratio of GumB-GumC to GumE. Therefore, when this ratio is higher than in wild-type bacteria, a shift toward the polymerization of longer chains occurs. Conversely, a decrease in the ratio of GumB-GumC to GumE produces shorter polymer chains, as observed for the decrease in xanthan viscosity in the parental strain containing additional copies of *gumE* (pBBad-E).

It is likely that protein–protein interactions between these three components of the polysaccharide polymerization and translocation machinery play an essential role in modulating polymer chain length. Additional experiments are needed to study the formation of a complex between the GumB, GumC and GumE proteins. At present, we obtained controversial results about the interaction between GumB and GumC. Co-elution of both proteins on ion-exchange and size exclusion chromatographies, after extracting them from bacterial membranes, suggested the formation of multimeric complexes that involved GumB and GumC. However, in vivo cross-linking experiments with different agents (i.e., formaldehyde, dithiobis[succinimidyl propionate]) and co-immunoprecipitation assays with anti-GumB and anti-GumC antibodies failed to detect a GumB–GumC interaction. Current work in our laboratory is aimed at exploring protein-protein interactions with purified proteins. Thus, GumB without its signal peptide was recently purified and crystallized (Jacobs et al. 2012). Understanding how GumB, GumC and GumE interplay to polymerize and export xanthan will help to better explain the mechanisms that govern polymer chain length regulation of this exopolysaccharide.

Materials and methods

Bacteria, plasmids and growth conditions

Strains and plasmids used in this study are listed in Table II. *X. campestris* strains were routinely grown in YM broth (Harding et al. 1993) at 28°C. For xanthan production, *X. campestris* cells were grown in an optimized media, XOL-SSF (4% sucrose, 1% K_2HPO_4, 0.02% KH_2PO_4, 0.01% $MgCl_2$, 0.0001% $MnCl_2$, 0.1% $(NH_4)_2SO_4$, 0.005% $FeSO_4$, 0.125% tryptone and 0.125% yeast extract in tap water, pH 7), at 28°C. Antibiotics were obtained from Sigma (St. Louis, Mo.) and were added to the media as required at the following concentrations (in micrograms per milliliter): Tetracycline, 10; kanamycin, 50; and gentamicin, 30. Arabinose was obtained from Sigma.

Bioinformatic analyses

To search for putative open reading frames, the open-reading frame (ORF) Finder software from Clone Manager 7, v.7.11 software (Scientific & Educational Software, NC) was used. The predictions of protein localization were made with PSORTb v3.0.2 software (Yu et al. 2010), and the predictions of transmembrane regions were made using TMHMM v.2.0 software (Sonnhammer et al. 1998; Krogh et al. 2001). Prediction of lipoprotein signal sequence was performed using LipoP 1.0 software (Juncker et al. 2003). Amino acid homologies were detected using PSI-BLAST (Altschul et al. 1997).

Correction of the gumB *sequence*. We isolated and sequenced the *gumB* DNA region from *X. campestris* FC2 (XcFC2) cells. Our sequence (GenBank: AF427012) differed from the sequence reported by Capage et al. (1987) (GenBank: U22511); we found a deletion at nucleotide position 1299 and an inversion of nucleotides at positions 1301 and 1302 (the original CGTCGC sequence should be changed to CTGCC). This difference resulted in a frameshift that caused an N-terminal extension of 19-residues in GumB. Our corrected GumB sequence (GenBank: AAL28080) predicted a prolipoprotein of 232 amino acid and an MW of 25.30 kDa.

Correction of the gumC *sequence*. We sequenced the intergenic region between *gumB* and *gumC* from XcFC2 cells, and we found a difference in one base (GenBank: AF427011) at position 2012, where the reported G (GenBank: U22511) was not present in our new sequence. The absence of this base generated a shift in the open reading frame upstream of the previously described ATG. Our new GumC sequence (GenBank: AAL28079) has 23 additional amino acids at the N-terminus, a total length of 472 amino acids and an MW of 52.97 kDa.

Western blotting analysis

Proteins from whole bacteria or membrane preparations were solubilized with 2× denaturing buffer (10 M urea, 3% SDS, 0.4 M dithiothreitol and 100 mM Tris–HCl, pH 8.8), separated by sodium dodecyl SDS–PAGE in gels containing 10% acrylamide, transferred to polyvinylidene difluoride membrane, and probed in 3% nonfat dry milk with a specific antiserum (anti-GumB at 1:2000, anti-GumC at 1:5000, or anti-OprF at 1:1000). Polyclonal anti-GumB and anti-GumC antibodies were obtained in our laboratory, as described in the Supplementary Methods section, and Anti-OprF was generously provided by Dr. Gilleland's lab. Alkaline phosphatase-conjugated, goat anti-mouse IgG or goat anti-rabbit IgG antibodies (Gibco-BRL) were used as secondary antibodies, and detection was performed with a BCIP/NBT color development substrate (Promega, Madison, WI). Quantification of the proteins detected by western blotting was performed with the ImageJ 1.43u software (National Institutes of Health). For each protein, we arbitrarily assigned a value of 1.0 to the protein expression observed in wild-type cells carrying the empty vector (XcFC2/pBBad22k). The signal intensities obtained for both GumB and GumC on strain Xc3192 carrying the empty vector were comparable with the corresponding signals observed on XcFC2/pBBad22k. To standardize for blot/signal variation, a control lane with the strain used as reference (XcFC2/pBBad22k or Xc3192/pBBad22k) was included in each blot. Analysis of the signal intensities obtained when increasing amounts of XcFC2/pBBad22k

membranes were subjected to western blotting showed that we were able to detect up to 8-fold increase in signal intensity without saturating the detection system, for both GumB and GumC proteins.

Cell fractionation and membrane sedimentation analysis

Total membranes and soluble fractions were obtained as described by Barreras et al. (2000). Briefly, *X. campestris* cells were broken using a French pressure cell press; unbroken cells were removed by centrifugation. The lysate was subjected to ultracentrifugation to separate the total membrane fraction from the soluble fraction. The presence of GumB and GumC in both fractions was analyzed by western blotting. IM and OM were separated using discontinuous sedimentation sucrose gradients, following the technique described for *X. campestris* (Dianese and Schaad 1982). The XcFC2 total membrane fraction was layered on the top of a 45–70% sucrose gradient. The gradient was centrifuged at 110,000 × *g* for 4 h, and 1-mL fractions were collected. The efficacy of the membrane isolation procedure was confirmed by measuring the activity of NADH oxidase (Orndorff and Dworkin 1980) and the content of 2-keto 3-deoxyoctanoic acid (Gerhardt 1994). The composition of these fractions was also analyzed by western blotting with anti-GumB and anti-GumC polyclonal antibodies.

Globomycin treatment

XcFC2 cells were grown to an optical density at 600 nm (OD_{600}) of ~0.4–0.8 before 180 µg/mL of globomycin (obtained from Dr. Masatoshi Inukai) was added to the medium. After incubation at different time points, cells were harvested, solubilized with 2× denaturing buffer, and analyzed by western blotting with the anti-GumB antibody.

Construction of X. campestris *mutants*

In a previous work (Katzen et al. 1998), the inactivation of *gumB*, *gumC* and *gumE* in the wild-type strain XcFC2 appeared to be lethal; the accumulation of certain toxic, lipid-linked intermediates might be responsible for that effect. However, mutants in the *gumB*, *gumC* and *gumE* genes were obtained in strain Xc3192, which is deficient in UDP-glucose pyrophosphorylase. These mutants exhibited an additional defect that involved GumD activity, which is responsible for the transfer of glucose-1-phosphate from UDP-glucose to polyisopreny lphosphate. To solve this inconvenience, new mutants were constructed. For the generation of the GumB-deficient strain, an Xc3192 subclone (UDP-glucose pyrophosphorylase activity deficient, $gumD^{+}$) was used. The *gumB* mutant, Xc3192B, was generated by integrating the suicide plasmid, pGum57-18S, into the Xc3192 strain following the technique described by Katzen et al. (1998). The *gumC* mutant strain Xc3192C was made as a transcriptional fusion mutant using the nonpolar, promoterless *gumC-lacZ-aacC1* interposon, which was inserted in the same direction as the proposed *gumC* open reading frame (Katzen et al. 1996). Strains Xc3192BC (a deletion mutant for both *gumB* and *gumC*) and Xc3192E (a 500 bp internal deletion of *gumE*) were constructed following the technique described by Coleman et al. (2008). To construct a *gumBgumC* double mutant strain, two DNA fragments of 1 kb flanking the *gumBC* region were amplified by Polymerase chain reaction (PCR) with primer pairs FwUpB_*Sph*I (5′-ACATGCATGCAGGAACGGGTGGAGGCTTATCG-3′) and RvUpB_*Sal*I (5′-ACTGTCGACGCGTGTAGCTGGCTGCCTCTGTTG-3′) and FwDownC_*Sal*I (5′-ACGCGTCGACCATCGTGATGTTGCAAAACG-3′) and RvDownC_*Xma*I (5′-TCCCCCCGGGCACCAGCTTCACGTTG-3′), respectively. These two PCR fragments were cloned into pTR213b (CP Kelco), a pK18mobGII (Katzen et al. 1999) derivative plasmid carrying the *Bacillus subtilis sacB* gene and generating plasmid pTR-BC. To generate a *gumE* deletion mutant, plasmid pTR-E was constructed by cloning a *Pst*I fragment of 2204 bp (nt 4523–6728) containing *gumE* with an internal deletion of 509 bp (nt 5629–6138) into pTR213b. To delete the *gumBgumC* or *gumE* genes from Xc3192, pTR-BC or pTR-E were electroporated into Xc3192 cells. Insertion of the plasmid into the chromosome was selected by kanamycin resistance. After growth without antibiotics, recombinants were isolated by selecting for loss of sucrose toxicity conferred by the *sacB* gene. All gene deletions were confirmed by PCR using the appropriate primers. None of the mutants we constructed (Xc3192B, Xc3192C, Xc3192BC or Xc3192E) showed any alteration in their in vitro ability to synthesize the lipid-linked pentasaccharide (Katzen et al. 1998), as shown in Table I.

Plasmid constructions

(**i**) pBBad-B. The extended ORF for *gumB* (GenBank: AF427012) was amplified from the genome of XcFC2 cells using the primers FwB (5′- CATGCCATGGGGAAGAAACTCATCGGACGACTCTGC-3′) and RvB (5′- CCCAAGCTTTCATCGGTAAGCGCGCCAC). The PCR product was digested with *Nco*I and *Hind*III and ligated to the corresponding sites of pBBad22T to yield plasmid pBBad-B. (**ii**) pBBad-C. To generate pBBad-C, the *gumC* gene (GenBank: AF427011) was amplified from the genome of XcFC2 cells using the primers FwC (5′-CCATGGGGAATTCAGACAATCGTTCCTCTTCG-3′) and RvC (5′-GGGAAGCTTTCAGTTCAACCGCGACCTCGGAGAAGGCCC-3′). The PCR products were digested with *Nco*I and *Hind*III and ligated to the corresponding sites of pBBad22K. (**iii**) pBBad-BC. Plasmid pBBad-BC was obtained as described for pBBad-C using the primers FwB and RvC. (**iv**) pBBad-E. The *gumE* gene carrying a C-terminal His_6 tag was amplified from XcFC2 using the primers FwE (5′-CGCCC*ATGG*GACTGATTCAAATGAGCGAG-3′) and RvE (5′-CCCAAGCTTTCAATGATGATGATGATGCCGCGGCGCTCC-3′). The PCR product was digested with *Nco*I and *Hind*III and ligated to the corresponding sites of pBBad22K to yield plasmid pBBad-E. (**v**) pBBR-promB. For the construction of the pBBR-promB plasmid, a 2855 bp fragment was released from plasmid pGum02-19S (Katzen et al. 1996) by digestion with *Sph*I and then cloned into pUC18 (Yanisch_Perron et al. 1985), forming pUC18-BC_AS. The *Hind*III-*Xba*I fragment released from pUC18-BC_AS containing the *gum* promoter and the *gumB* gene was cloned into the pBBR1MCS-5 plasmid to yield pBBR-promB. (**vi**) pBBR-prom. A 276 bp fragment including the *gum* operon promoter region and carrying an ATG

codon 12 bp downstream of the RBS by adding an *Nde*I restriction site was generated by PCR from *X. campestris* chromosomal DNA using the specific oligonucleotides Uprom (5′-ACATGCATGCGCTAGAGTTCGTATGCTGAGAAT-3′) and Lprom (5′-ACATGCATGCCATATGTGTAGCTGGCTGCCTCTG-3′). This fragment was cloned into pBBR1-MCS-5, generating pBBR-prom. (**vii**) pBBR-promB_{22511}. To construct the pBBR-promB_{22511} plasmid, a 642 bp fragment coding for the previously described *gumB* gene (GenBank: U22511) was amplified by PCR using oligonucleotides UB_{22511} (5′-GGAATTCCATATGTCGCTGGGCGCTTGCAG-3′) and LB_{22511} (5′-CGGAATTCTCATCGGTAAGCGCGCCACAC-3′). The PCR product was digested with *Nde*I and *EcoR*I and ligated to the corresponding sites of pBBR-prom, generating pBBR-promB_{22511}. (**viii**) pBBR-promC. The extended *gumC* ORF (GenBank AF427012) was amplified from *X. campestris* chromosomal DNA using specific oligonucleotides UgumC (5′-GGATTCCATATGAATTCAGACAATCGTTCCTC-3′) and LgumC (5′-CGGGGTACCTCAGTTCAACCGCGACCTC-3′). The PCR product was digested with *Nde*I and *Kpn*I and ligated to the corresponding sites of pBBR-prom to yield plasmid pBBR-promC. (**ix**) pBBad-C_{22511}. Plasmid pBBad-C_{22511}, which carries the previously reported *gumC* gene (GenBank U22511), was obtained as described for pBBad-C, using primers UgumC_{22511} (5′-GGATTCCATATGGACTACTGGCGCCGCCCTG-3′) and LgumC.

In vitro xanthan biosynthesis

In vitro determinations of lipid-linked intermediates and xanthan biosynthesis were performed as previously reported (Katzen et al. 1998). Briefly, EDTA-permeabilized *X. campestris* cells were incubated with UDP-glucose, GDP-mannose and UDP-[^{14}C]glucuronic acid and then centrifuged. Pellets were extracted with chloroform:methanol:water (1:2:0.3, vol vol^{-1}) and analyzed by paper chromatography to determine the synthesis of the lipid-linked pentasaccharide repeating units. Supernatants, which contained the polymerization products, were analyzed by gel filtration chromatography on a Bio-Gel A-5 m.

In vivo xanthan production and viscosity determinations

For xanthan production, *X. campestris* cells were grown in XOL-SSF media at 28°C and, when indicated, arabinose was added to cultures with an $OD_{600} \sim 0.7$. After 96 h, xanthan was precipitated with two volumes of isopropanol and recovered by filtration on a stainless-steel sieve. Wet xanthan fibers were washed with increasing concentrations of ethanol (75–100% ethanol in water), dried at 55°C and weighed to determine xanthan yield. Low shear rate viscosity was determined for a 0.45% xanthan solution in synthetic tap water (16.2 mM NaCl, 0.95 mM $CaCl_2$) at ambient temperature using a Brookfield viscometer (RVTD II) with spindle no. 1 at 3 rpm. Intrinsic viscosity measurements of xanthan solutions in 0.05 M NaCl were performed using the Vilastic Viscoelasticity Analyzer (Vilastic Scientific, Inc., Austin, TX).

Atomic force microscopy and contour length determination

A commercial atomic force microscope (Bruker – DI multimode Nanoscope IIIa) was employed to measure xanthan contour length under ambient conditions using a silicon nitride cantilever tip (Nano Devices, Veeco Metrology, Santa Barbara, CA; pyramidal tip shape; cone half angle $a = 18°$; tip curvature radius $r = 2$ nm; resonant frequency nominal: 120 kHz; measured: 101.5 kHz; and spring constant: 0.5 N m^{-1}). A xanthan dispersion (5 µL of 1.0 ng per mL solution in 0.1 M ammonium acetate) was sprayed onto a freshly cleaved mica disc (1 cm^2), which was then placed in a heated chamber (60°C) for 1 h to remove excess of water. For each condition, contour lengths of at least 500 macromolecules were measured with the ImageJ 1.43 u software (National Institutes of Health).

Supplementary data

Supplementary data for this article are available online at http://glycob.oxfordjournals.org/.

Funding

This work was supported by grants from the Agencia Nacional de Promoción Científica y Técnológica (ANPCyT) [PICT 1/2452] (Argentina); the National Research Council (CONICET) [PIP 399] (Argentina); and CP Kelco (L.I.). M.I.B. is a postdoctoral fellow of ANPCyT, E.A.F. is a doctoral fellow of CONICET and E.M.G. and L.I. are Career Investigators for CONICET (Argentina).

Conflict of interest

None declared.

Acknowledgements

We are grateful to Masatoshi Inukai (Sankyo, Japan) for providing globomycin and Harry E. Gilleland (Ohio State University, OH) for providing the anti-OprF antibody. We also thank Horacio Corti (Comisión Nacional de Energia Atomica, Buenos Aires, Argentina) for his help with AFM, Marta Bravo and Jimena Ortega (Instituto Leloir) for their technical assistance with DNA sequencing, Mariana Gallo and Daniel O. Cícero (Instituto Leloir) for their assistance with the NMR experiments, Dan Burgum (CP Kelco) for his assistance with the intrinsic viscosity determinations and Nancy E. Harding (CP Kelco) for critically reviewing the manuscript.

Abbreviations

BLAST, Basic Local Alignment Search Tool; CPS, capsular polysaccharides; EDTA, Ethylenediaminetetraacetic acid; EPS, produces an exopolysaccharide; GDP, guanine diphosphate; IgG, goat anti-mouse; IM, inner membrane; KDO, 2-keto 3-deoxyoctanoic acid; LPS O-Ag, lipopolysaccharide O-antigen; LSRV, Low shear rate viscosities; NMR, nuclear magnetic resonance; OM, outer membrane; OPX, outer membrane polysaccharide export; ORF, open reading frames; PCP, polysaccharide co-polymerase; PCR, Polymerase chain reaction; PES, polysaccharide export sequence; SDS–PAGE,

sodium dodecyl sulfate–polyacrylamide gel electrophoresis; UDP, uridine diphosphate.

References

Altschul SF, Madden TL, Schaffer AA, Zhang J, Zhang Z, Miller W, Lipman DJ. 1997. Gapped BLAST and PSI-BLAST: A new generation of protein database search programs. *Nucleic Acids Res*. 25:3389–3402.

Barreras M, Abdian PL, Ielpi L. 2004. Functional characterization of GumK, a membrane-associated beta-glucuronosyltransferase from *Xanthomonas campestris* required for xanthan polysaccharide synthesis. *Glycobiology*. 14:233–241.

Barreras M, Salinas SR, Abdian PL, Kampel MA, Ielpi L. 2008. Structure and mechanism of GumK, a membrane-associated glucuronosyltransferase. *J Biol Chem*. 283:25027–25035.

Becker A, Vorholter FJ. 2009. Xanthan Biosynthesis by *Xanthomonas* Bacteria: An Overview of the Current Biochemical and Genomic Data. In: Rehm BHA, editor. *Microbial Production of Biopolymers and Polymer Precursors: Applications and Perspectives*. Norfolk, UK: Caister Academic Press. p. 1–12.

Cadmus MC, Rogovin SP, Burton KA, Pittsley JE, Knutson CA, Jeanes A. 1976. Colonial variation in *Xanthomonas campestris* NRRL B-1459 and characterization of the polysaccharide from a variant strain. *Can J Microbiol*. 22:942–948.

Capage MR, Doherty DH, Betlach MR, Vanderslice RW. 1987. Recombinant-DNA mediated production of xanthan gum. International patent International patent WO87/05938: B.

Carter JA, Jimenez JC, Zaldivar M, Alvarez SA, Marolda CL, Valvano MA, Contreras I. 2009. The cellular level of O-antigen polymerase Wzy determines chain length regulation by WzzB and WzzpHS-2 in *Shigella flexneri* 2a. *Microbiology*. 155:3260–3269.

Coleman RJ, Patel YN, Harding NE. 2008. Identification and organization of genes for diutan polysaccharide synthesis from *Sphingomonas* sp. ATCC 53159. *J Ind Microbiol Biotechnol*. 35:263–274.

Collins RF, Beis K, Clarke BR, Ford RC, Hulley M, Naismith JH, Whitfield C. 2006. Periplasmic protein-protein contacts in the inner membrane protein Wzc form a tetrameric complex required for the assembly of *Escherichia coli* group 1 capsules. *J Biol Chem*. 281:2144–2150.

Collins RF, Beis K, Dong C, Botting CH, McDonnell C, Ford RC, Clarke BR, Whitfield C, Naismith JH. 2007. The 3D structure of a periplasm-spanning platform required for assembly of group 1 capsular polysaccharides in *Escherichia coli*. *Proc Natl Acad Sci USA*. 104:2390–2395.

Cuthbertson L, Mainprize IL, Naismith JH, Whitfield C. 2009. Pivotal roles of the outer membrane polysaccharide export and polysaccharide copolymerase protein families in export of extracellular polysaccharides in gram-negative bacteria. *Microbiol Mol Biol Rev*. 73:155–177.

Daniels C, Vindurampulle C, Morona R. 1998. Overexpression and topology of the *Shigella flexneri* O-antigen polymerase (Rfc/Wzy). *Mol Microbiol*. 28:1211–1222.

Dianese JC, Schaad NW. 1982. Isolation and characterization of inner and outer membranes of *Xanthomonas campestris* pv. *campestris*. *Phytopathology*. 72:1284–1289.

Dong C, Beis K, Nesper J, Brunkan-Lamontagne AL, Clarke BR, Whitfield C, Naismith JH. 2006. Wza the translocon for *E. coli* capsular polysaccharides defines a new class of membrane protein. *Nature*. 444:226–229.

Dow JM, Crossman L, Findlay K, He YQ, Feng JX, Tang JL. 2003. Biofilm dispersal in *Xanthomonas campestris* is controlled by cell-cell signaling and is required for full virulence to plants. *Proc Natl Acad Sci USA*. 100:10995–11000.

Drummelsmith J, Whitfield C. 2000. Translocation of group 1 capsular polysaccharide to the surface of *Escherichia coli* requires a multimeric complex in the outer membrane. *EMBO J*. 19:57–66.

Gerhardt P. 1994. *Methods for General and Molecular Bacteriology*. Washington, D.C: American Society for Microbiology.

Guo H, Yi W, Song JK, Wang PG. 2008. Current understanding on biosynthesis of microbial polysaccharides. *Curr Top Med Chem*. 8:141–151.

Harding NE, Raffo S, Raimondi A, Cleary JM, Ielpi L. 1993. Identification, genetic and biochemical analysis of genes involved in synthesis of sugar nucleotide precursors of xanthan gum. *J Gen Microbiol*. 139:447–457.

Hiemenz PC, Lodge TP. 2007. *Polymer Chemistry*. New York: Marcel Dekker, Inc. p. 338–339.

Huang J, Schell M. 1995. Molecular characterization of the eps gene cluster of *Pseudomonas solanacearum* and its transcriptional regulation at a single promoter. *Mol Microbiol*. 16:977–989.

Ielpi L, Couso RO, Dankert MA. 1993. Sequential assembly and polymerization of the polyprenol-linked pentasaccharide repeating unit of the xanthan polysaccharide in *Xanthomonas campestris*. *J Bacteriol*. 175:2490–2500.

Inukai M, Takeuchi M, Shimizu K, Arai M. 1978. Mechanism of action of globomycin. *J Antibiot (Tokio)*. 31:1203–1205.

Jacobs M, Salinas SR, Bianco MI, Ielpi L. 2012. Expression, purification and crystallization of the outer membrane lipoprotein GumB from *Xanthomonas campestris*. *Acta Crystallogr Sect F Struct Biol Cryst Commun*. 68:1255–1258.

Jansson PE, Kenne L, Lindberg B. 1975. Structure of extracellular polysaccharide from *Xanthomonas campestris*. *Carbohydr Res*. 45:275–282.

Juncker AS, Willenbrock H, Von Heijne G, Brunak S, Nielsen H, Krogh A. 2003. Prediction of lipoprotein signal peptides in Gram-negative bacteria. *Protein Sci*. 12:1652–1662.

Kanegasaki S, Wright A. 1970. Mechanism of polymerization of the *Salmonella* O-antigen: Utilization of lipid-linked intermediates. *Proc Natl Acad Sci USA*. 67:951–958.

Katzen F, Becker A, Ielmini MV, Oddo CG, Ielpi L. 1999. New mobilizable vectors suitable for gene replacement in gram-negative bacteria and their use in mapping of the 3′ end of the *Xanthomonas campestris* pv. *campestris gum* operon. *Appl Environ Microbiol*. 65:278–282.

Katzen F, Becker A, Zorreguieta A, Puhler A, Ielpi L. 1996. Promoter analysis of the *Xanthomonas campestris* pv. *campestris* gum operon directing biosynthesis of the xanthan polysaccharide. *J Bacteriol*. 178:4313–4318.

Katzen F, Ferreiro DU, Oddo CG, Ielmini MV, Becker A, Puhler A, Ielpi L. 1998. *Xanthomonas campestris* pv. *campestris* gum mutants: Effects on xanthan biosynthesis and plant virulence. *J Bacteriol*. 180:1607–1617.

Kintz EN, Goldberg JB. 2011. Site-directed mutagenesis reveals key residue for O antigen chain length regulation and protein stability in *Pseudomonas aeruginosa* Wzz2. *J Biol Chem*. 286:44277–44284.

Kovach ME, Elzer PH, Hill DS, Robertson GT, Farris MA, Roop RM, Peterson KM. 1995. Four new derivatives of the broad-host-range cloning vector pBBR1MCS, carrying different antibiotic-resistance cassettes. *Gene*. 166:175–176.

Krogh A, Larsson B, von Heijne G, Sonnhammer EL. 2001. Predicting transmembrane protein topology with a hidden Markov model: Application to complete genomes. *J Mol Biol*. 305:567–580.

Marczak M, Mazur A, Krol JE, Gruszecki WI, Skorupska A. 2006. Lipoprotein PssN of *Rhizobium leguminosarum* bv. *trifolii*: Subcellular localization and possible involvement in exopolysaccharide export. *J Bacteriol*. 188: 6943–6952.

Mazur A, Krol JE, Wielbo J, Urbanik-Sypniewska T, Skorupska A. 2002. *Rhizobium leguminosarum* bv. *trifolii* PssP protein is required for exopolysaccharide biosynthesis and polymerization. *Mol Plant Microbe Interact*. 15:388–397.

Morona R, Van Den Bosch L, Daniels C. 2000. Evaluation of Wzz/MPA1/MPA2 proteins based on the presence of coiled-coil regions. *Microbiology*. 146(Pt 1):1–4.

Morona R, van den Bosch L, Manning PA. 1995. Molecular, genetic, and topological characterization of O-antigen chain length regulation in *Shigella flexneri*. *J Bacteriol*. 177:1059–1068.

Nakar D, Gutnick DL. 2003. Involvement of a protein tyrosine kinase in production of the polymeric bioemulsifier emulsan from the oil-degrading strain *Acinetobacter lwoffii* RAG-1. *J Bacteriol*. 185:1001–1009.

Orndorff PE, Dworkin M. 1980. Separation and properties of the cytoplasmic and outer membranes of vegetative cells of *Myxococcus xanthus*. *J Bacteriol*. 141:914–927.

Patel YN, Schneider JC, Ielpi L, Ielmini MV. 2008. *High Viscosity Xanthan Polymer Preparations*. US: 7,439,044 B2.

Paulsen IT, Beness AM, Saier MH, Jr. 1997. Computer-based analyses of the protein constituents of transport systems catalysing export of complex carbohydrates in bacteria. *Microbiology*. 143(Pt 8):2685–2699.

Raetz CR, Whitfield C. 2002. Lipopolysaccharide endotoxins. *Annu Rev Biochem*. 71:635–700.

Reid AN, Whitfield C. 2005. functional analysis of conserved gene products involved in assembly of *Escherichia coli* capsules and exopolysaccharides: Evidence for molecular recognition between Wza and Wzc for colanic acid biosynthesis. *J Bacteriol*. 187:5470–5481.

Reuber TL, Walker GC. 1993. Biosynthesis of succinoglycan, a symbiotically important exopolysaccharide of *Rhizobium meliloti*. *Cell*. 74:269–280.

Salinas SR, Bianco MI, Barreras M, Ielpi L. 2011. Expression, purification and biochemical characterization of GumI, a monotopic membrane GDP-mannose: glycolipid 4-{beta}-D-mannosyltransferase from *Xanthomonas campestris* pv. *campestris*. *Glycobiology*. 21:903–913.

Sonnhammer EL, von Heijne G, Krogh A. 1998. A hidden Markov model for predicting transmembrane helices in protein sequences. *Proc Int Conf Intell Syst Mol Biol*. 6:175–182.

Stankowski JD, Mueller BE, Zeller SG. 1993. Location of a second O-acetyl group in xanthan gum by the reductive-cleavage method. *Carbohydr Res*. 241:321–326.

Stevenson G, Andrianopoulos K, Hobbs M, Reeves PR. 1996. Organization of the *Escherichia coli* K-12 gene cluster responsible for production of the extracellular polysaccharide colanic acid. *J Bacteriol*. 178:4885–4893.

Sukchawalit R, Vattanaviboon P, Sallabhan R, Mongkolsuk S. 1999. Construction and characterization of regulated L-arabinose-inducible broad host range expression vectors in *Xanthomonas*. *FEMS Microbiol Lett*. 181:217–223.

Tao F, Swarup S, Zhang LH. 2010. Quorum sensing modulation of a putative glycosyltransferase gene cluster essential for *Xanthomonas campestris* biofilm formation. *Environ Microbiol*. 12:3159–3170.

Tocilj A, Munger C, Proteau A, Morona R, Purins L, Ajamian E, Wagner J, Papadopoulos M, Van Den Bosch L, Rubinstein JL, et al. 2008. Bacterial polysaccharide co-polymerases share a common framework for control of polymer length. *Nat Struct Mol Biol*. 15:130–138.

Tokuda H. 2009. Biogenesis of outer membranes in Gram-negative bacteria. *Biosci Biotechnol Biochem*. 73:465–473.

Vojnov AA, Zorreguieta A, Dow JM, Daniels MJ, Dankert MA. 1998. Evidence for a role for the gumB and gumC gene products in the formation of xanthan from its pentasaccharide repeating unit by *Xanthomonas campestris*. *Microbiology*. 144(Pt 6):1487–1493.

Vorholter FJ, Schneiker S, Goesmann A, Krause L, Bekel T, Kaiser O, Linke B, Patschkowski T, Ruckert C, Schmid J, et al. 2008. The genome of *Xanthomonas campestris* pv. *campestris* B100 and its use for the reconstruction of metabolic pathways involved in xanthan biosynthesis. *J Biotechnol*. 134:33–45.

Woodward R, Yi W, Li L, Zhao G, Eguchi H, Sridhar PR, Guo H, Song JK, Motari E, Cai L, et al. 2010. In vitro bacterial polysaccharide biosynthesis: Defining the functions of Wzy and Wzz. *Nat Chem Biol*. 6:418–423.

Wugeditsch T, Paiment A, Hocking J, Drummelsmith J, Forrester C, Whitfield C. 2001. Phosphorylation of Wzc, a tyrosine autokinase, is essential for assembly of group 1 capsular polysaccharides in *Escherichia coli*. *J Biol Chem*. 276:2361–2371.

Yanisch_Perron C, Vieira J, Messing J. 1985. Improved M13 phage cloning vectors and host strains: Nucleotide sequences of the M13mp18 and pUC19 vectors. *Gene*. 33:103–119.

Yu NY, Wagner JR, Laird MR, Melli G, Rey S, Lo R, Dao P, Sahinalp SC, Ester M, Foster LJ, et al. 2010. PSORTb 3.0: Improved protein subcellular localization prediction with refined localization subcategories and predictive capabilities for all prokaryotes. *Bioinformatics*. 26: 1608–1615.

Yun MH, Torres PS, El Oirdi M, Rigano LA, Gonzalez-Lamothe R, Marano MR, Castagnaro AP, Dankert MA, Bouarab K, Vojnov AA. 2006. Xanthan induces plant susceptibility by suppressing callose deposition. *Plant Physiol*. 141:178–187.